Power statistics of Otto heat engines with the Mpemba effect

Jie Lin,[1] Kai Li,[1] Jizhou He,[1] Jie Ren,[2,*] and Jianhui Wang[1,3,†]

[1]*Department of Physics, Nanchang University, Nanchang 330031, China*

[2]*Center for Phononics and Thermal Energy Science, China-EU Joint Lab on Nanophononics, Shanghai Key Laboratory of Special Artificial Microstructure Materials and Technology, School of Physics Sciences and Engineering, Tongji University, Shanghai 200092, China*

[3]*State Key Laboratory of Surface Physics and Department of Physics, Fudan University, Shanghai 200433, China*

(Received 12 June 2021; revised 7 December 2021; accepted 14 December 2021; published 4 January 2022)

The Mpemba effect is a counterintuitive relaxation phenomenon whereby a system with a higher initial temperature may cool down to the thermal state faster than an identical system that was initially prepared at a lower temperature. Here, we investigate heat and work in a Markovian state transition system with cyclic switching hot-cold temperatures, which operates as an Otto heat engine working in long but finite time, either with or without the Mpemba effect. Under the condition of the periodic steady state having been reached, the time durations of the heating and cooling relaxation processes are determined by exploring a distance-from-equilibrium equivalent to the Kullback-Leibler divergence. We then numerically evaluate and compare the averages and variances of both the work and the power output of two scenarios with and without the Mpemba effect. The results show that the Markovian Mpemba effect can enhance the machine performance by significantly increasing the power output for a given efficiency without sacrificing the stability.

DOI: 10.1103/PhysRevE.105.014104

I. INTRODUCTION

A heat engine that operates with a classical or quantum system working between a hot and a cold reservoir is a topic of great interest. Apart from its potential application in energy utilization, a heat engine in finite time provides a good platform for understanding the nonequilibrium thermodynamics and statistics of the system. The heat engines from the microscale to the macroscale have been extensively investigated, with strong emphasis on performance optimization when these engines produce finite power [1–12]. Owing to nonnegligible fluctuations [12–23] of heat and work in finite-size systems, for heat engines at the microscale and the mesoscale, the power output is a stochastic variable, and the power fluctuations characterizing the instability of engines [24] should be considered. Previous studies have shown that the increase of power leads to the increase of power fluctuations owing to the trade-off between them, for either steady-state [25,26] or cyclic [18,24] engine models. Therefore, it is worthwhile to consider the power fluctuations as a figure of merit wherein both the performance measure and the stability of the thermal machines are involved.

Typically, it is expected that a system prepared at a cold temperature cools down faster compared with an identical system initiated at a hot temperature when both are cooled to a colder reservoir. Although this is typically true, it is not always the case, and a hot system may cool down faster compared with a cold system. This anomalous cooling effect is called the Mpemba effect (ME) [27–29], and its phenomenological description [30] was recently proposed within the context of Markovian dynamics. However, the underlying mechanism for the occurrence of the Mpemba effect remains elusive owing to its complexity [31,32]. Recent studies have proposed that Mpemba-like behavior may be observed in various systems [30,32–42], including small systems [30,32] that can be satisfactorily described by stochastic thermodynamics. Since the performance in the finite time of heat engines is sensitive to the working substance, a question naturally arises with regard to whether the performance of finite-time heat engines can be enhanced by the ME. To answer this question, we analyze an Otto engine by adopting a three-state system as the working substance, where ME (inverse ME) could occur along the cooling (heating) process, assuming that the engine (with long but not infinite cycle duration) has reached a periodic steady state.

To model an Otto engine cycle [43–47] consisting of two isochoric and two adiabatic processes, this study adopts two different three-state systems: one exhibits the ME, while the other does not. The numerical calculations show that, for a given thermodynamic efficiency, the power output can be significantly enhanced by the ME without sacrificing the engine stability. The rest of this paper is organized as follows. In Sec. II, following the approach adopted in Ref. [30], the distance-from-equilibrium is numerically investigated to determine the time duration along an isochoric cooling process, in both the presence and the absence of ME. The distance-from-equilibrium is shown to be identical to the Kullback-Leibler divergence. The performance analysis is presented in Sec. III, wherein the effects induced by ME on the time cycle period, power, and relative power fluctuations are determined. Section IV summarizes the conclusions drawn from this study.

*Xonics@tongji.edu.cn

†wangjianhui@ncu.edu.cn

II. PHENOMENOLOGICAL DESCRIPTION OF MPEMBA EFFECT BY USING MARKOVIAN DYNAMICS

Following Ref. [30], the dynamics of a system in contact with an ideal thermal bath with a constant inverse temperature β^r ($k_B \equiv 1$, $\beta^r = 1/T_r$) can be determined using the stochastic master equation [48]:

$$\frac{dp_n(t)}{dt} = \sum_m R_{nm} p_m(t), \quad n = 1, 2, 3, \ldots, \tag{1}$$

where $p_n(t)$ denotes the occupation probabilities for states n at time t, and R_{nm} is the element of the stochastic transition matrix that represents the transition rate from state m to state n. Elements R_{nm} depend on the energy (ε_m), the energy barrier between the states ($\mathcal{B}_{mn} = \mathcal{B}_{nm}$), and the inverse temperature of the thermal bath β^r. These elements take the Arrhenius form, as follows:

$$R_{nm} = \begin{cases} \gamma e^{-\beta^r(\mathcal{B}_{nm} - \varepsilon_m)}, & n \neq m, \\ -\sum_{l \neq m} R_{lm}, & n = m, \end{cases} \tag{2}$$

where γ is a constant. When the system achieves thermal equilibrium steady state, the occupation probabilities p_n must approach their equilibrium values π_n determined by the Boltzmann distribution, as follows: $\pi_n = e^{-\beta^r \varepsilon_n}/Z$, where $Z = \sum_n e^{-\beta^r \varepsilon_n}$ is the canonical partition function. In stochastic thermodynamics, the total entropy production rate of a system coupled to a heat bath can be obtained as follows:

$$\dot{S}(t) = \sum_{n<m} J_{mn} \ln \frac{R_{nm} p_m}{R_{mn} p_n}, \tag{3}$$

where $J_{nm} = R_{nm} p_m - R_{mn} p_n = -J_{mn}$, and thus J_{nm} denotes the net probability current from state m to state n. For a system at thermal equilibrium, $\overrightarrow{p}(t) = \overrightarrow{\pi}(\beta^r)$ and $R_{mn}\pi_n = R_{nm}\pi_m$, and the entropy production rate vanishes, that is, $\dot{S} = 0$.

To describe how far the system deviates from the thermal equilibrium, we explore the distance-from-equilibrium function $F[\overrightarrow{p}(t); \beta^r]$, which can be defined by integrating $\dot{S}$ from time t to ∞ [30] as $F[\overrightarrow{p}(t); \beta^r] = \int_t^\infty \dot{S}(t')dt'$. By inserting Eq. (3), one readily obtains

$$F[\overrightarrow{p}(t); \beta^r] = \sum_n [\beta^r \varepsilon_n (p_n - \pi_n) + p_n \ln p_n - \pi_n \ln \pi_n]. \tag{4}$$

This is a decreasing function of time t and vanishes at $t \to \infty$ since $\overrightarrow{p(t)}|_{t\to\infty} = \overrightarrow{\pi}(\beta^r)$. Alternatively, we can prove that this distance function is equivalent to the Kullback-Leibler divergence [49] (also called relative entropy, or information divergence) between the probability distributions $\overrightarrow{p}(t)$ and $\overrightarrow{\pi}$:

$$F[\overrightarrow{p}(t); \beta^r] = \sum_n p_n \ln(p_n/\pi_n), \tag{5}$$

since $\sum_n [\beta^r \varepsilon_n (p_n - \pi_n)] = \sum_n [-(p_n - \pi_n) \ln \pi_n]$ by using probability conservation $\sum_n p_n = \sum_n \pi_n = 1$.

Let us assume that two copies of the same system are prepared at two equilibrium states with inverse temperature β_a and $\beta_b > \beta_a$, respectively. Then, they are cooled by a cold heat bath with inverse temperature β^r, where $\beta^r > \beta_b > \beta_a$. If the ME holds in the system, the relationship $F[\overrightarrow{p}^a(t); \beta^r] < F[\overrightarrow{p}^b(t); \beta^r]$ should be satisfied for $t > t_v$, where t_v is the finite time length of the relaxation. In other words, when $t > t_v$, the distance from the equilibrium of the initially hotter system is smaller than that of the initially colder system owing to the ME. When the initial temperature is given for the system under consideration, the distance-from-equilibrium function (4) can be numerically determined by solving the master equation (1).

Let us consider two different three-state systems (cooled with a cold thermal bath), namely, $\mathcal{S}_1$ and $\mathcal{S}_2$, where $\mathcal{S}_1$ may exhibit the ME but $\mathcal{S}_2$ does not. A three-well potential energy landscape [Fig. 1(a)] is a mapping of these three states in the system with the transition rates sketched in Fig. 1(b). To determine the time duration of a relaxation process, we should consider the distance function (4) that indicates the distance from the thermal equilibrium.

The energy barriers $\mathcal{B}_{mn}(m \neq n)$ (with $m, n = 1, 2, 3$) are selected as follows: $\mathcal{B}_{12} = 1.5$, $\mathcal{B}_{13} = 0.8$, and $\mathcal{B}_{23} = 1.2$ in system $\mathcal{S}_1$ [30]; the energy barriers are $\mathcal{B}_{12} = 0.2$, $\mathcal{B}_{13} = 1.7$, and $\mathcal{B}_{23} = 1.9$ for system $\mathcal{S}_2$; the energies are the same $\varepsilon_1 = 0$, $\varepsilon_2 = 0.1$, and $\varepsilon_3 = 0.7$ for both systems $\mathcal{S}_1$ and $\mathcal{S}_2$. For two different initial temperature values, the distance function is plotted as a function of the time duration for systems $\mathcal{S}_1$ [Fig. 1(c)] and $\mathcal{S}_2$ [Fig. 1(d)]. At two different initial temperatures, system $\mathcal{S}_2$ evolves according to two non-overlapping paths toward the asymptotic thermal state $\pi(\beta^r)$, while the distance function of system $\mathcal{S}_1$ along the protocol of the higher initial temperature decays faster than that along the protocol of the lower initial temperature. Hence, ME is observed in system $\mathcal{S}_1$ but absent in system $\mathcal{S}_2$. Notably, regardless of the presence or absence of the ME, the distance function $F[\overrightarrow{p}(t); \beta^r]$ monotonically decreases as the interaction duration t increases and vanishes when the system reaches thermal equilibrium, as expected. For each initial inverse temperature β_i ($i = a$ and b), the relaxation time for the system that reaches thermal equilibrium is, in principle, determined by setting the distance function to zero. Importantly, a hotter system can cool down much faster owing to the ME, which motivates the implementation of a heat engine operating with a system wherein the ME is present.

III. PERFORMANCE ANALYSIS OF OTTO ENGINES

An Otto heat engine that works with the three-state system and consists of two isochoric and two adiabatic strokes is sketched in Fig. 1(e). The engine cycle consists of four consecutive steps, wherein the working system is alternatingly coupled to the two heat baths at inverse temperatures β_c^r and β_h^r, respectively.

(i) Cooling stroke $A \to B$. While being coupled to a cold thermal bath of constant inverse temperature β_c^r in a time period τ_c, the system with a fixed energy spectrum (i.e., constant energies ε_n^c) is releasing heat to the bath.

(ii) Adiabatic branch $B \to C$. The system with varying frequency is decoupled from the heat reservoir. Here, the adiabatic process is idealized as the sudden jumps of the potential, and therefore its time duration is negligible [50]. In this isentropic stroke, the occupation probabilities p_n remain constant owing to the constant entropy $S = -\sum_n p_n \ln p_n$. Hence, as the only variable of p_n, $\beta\varepsilon_n$ must be unvaried,

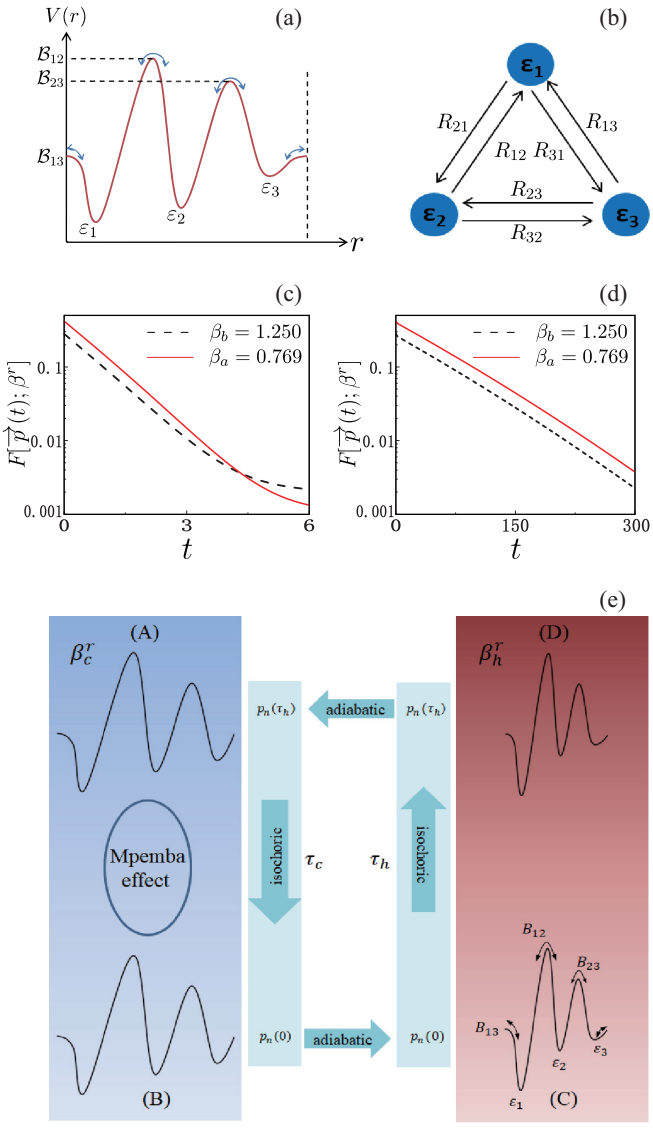

FIG. 1. (a) Sketch of three-well potential landscape with three states. (b) sketch of transition rates R_{mn} [Eq. (2)] in potential landscape as a three state system. Distance-from-equilibrium function of systems (c) $\mathcal{S}_1$ and (d) $\mathcal{S}_2$ versus time duration of system-bath interaction interval. A logarithmic scale is used for the distance function. For system $\mathcal{S}_1$, the energy barriers are $\mathcal{B}_{12} = 1.5$, $\mathcal{B}_{13} = 0.8$, and $\mathcal{B}_{23} = 1.2$; for system $\mathcal{S}_2$ the energy barriers are $\mathcal{B}_{12} = 0.2$, $\mathcal{B}_{13} = 1.7$, and $\mathcal{B}_{23} = 1.9$. Systems S_1 and S_2 both have the same energies: $\varepsilon_1 = 0$, $\varepsilon_2 = 0.1$, and $\varepsilon_3 = 0.7$. The inverse temperature of the cold thermal bath is $\beta_c^r = 5$. (e) Otto engine cycle consisting of a three-state system and working between a hot and a cold heat bath with inverse temperatures β_h^r and β_c^r.

which implies that the following relationship exists along this process: $\beta\varepsilon_n = \text{const}$.

(iii) Heating stroke $C \to D$. The system is weakly coupled to a hot heat reservoir at the inverse temperature β_h^r in the time duration τ_h, with constant energies $\varepsilon_n = \varepsilon_n^h$.

(iv) Adiabatic process $D \to A$. Again, by isolating the system from these two thermal baths, adiabatic compression in the sudden limit is performed to complete the cycle with the cycle period of $\tau_{\text{cyc}} = \tau_h + \tau_c$.

For isochoric cooling (i) and heating (iii), the system reaches the thermal equilibrium with the inverse temperature bath β_α^r ($\alpha = c$ and h) at the end of the stroke, if and only if the thermalization is complete with infinite τ_c or τ_h. However, owing to the finite time operation, the system of the cyclic engine in an isochoric stroke relaxes to the unique periodic steady state [51,52] (see the Appendix for details). As we show in the Appendix, when the two baths' inverse temperatures β_c^r and β_h^r are given, there are many periodic steady states for the Otto cycle, which are determined by setting F to be different non-negative values. In what follows, we consider one of these many periodic states that the heat engine under time-periodic driving has reached, which corresponds to the case when the distance function is much closer to zero and thus τ_c and τ_h are very long but not infinite. In such a periodic steady state, the system is close to thermal equilibrium at the end of each isochore.

Using the two-time measurement approach [12,18,22,23], the probability density function of the stochastic heat q_α along the isochoric stroke without produced work can be determined by the conditional probability to obtain the following equation:

$$p(q_\alpha) = \delta\left[q_\alpha - \left(\varepsilon_n^\alpha - \varepsilon_m^\alpha\right)\right] p_n(t_0) p_m(t_0 + \tau_\alpha), \tag{6}$$

where $p_n(t_0)$ is the probability of the system initially being in state n at time $t = t_0$, and $p_m(t_0 + \tau_\alpha)$ is the probability of the system collapsing into another state m after a time period τ_α with $\alpha = h$ and c. When the engine proceeds in finite time by cyclic driving, we are entering the periodic steady state $p_n(t_0 + \tau_c + \tau_h) = p_n(t_0)$. By considering Eq. (6), it follows that the average heat injection, $\langle q_\alpha \rangle = \int q_\alpha p(q_\alpha) dq_\alpha$, takes the following form:

$$\langle q_\alpha \rangle = \sum_n \varepsilon_n^\alpha [p_n(t_0) - p_n(t_0 + \tau_\alpha)]. \tag{7}$$

where $t_0 = 0$ for $\alpha = c$, and $t_0 = \tau_c$ for $\alpha = h$.

Work is done by the system during the adiabatic compression and expansion phases, whereas heat is exchanged with the two thermal baths during the isochoric branches. In other words, the work done by the system is equivalent to the total work produced along adiabatic trajectories (ii) and (iv), which leads to the following expression:

$$w[n(0); m(\tau_\alpha)] = \left(\varepsilon_n^h - \varepsilon_n^c\right) - \left(\varepsilon_m^h - \varepsilon_m^c\right), \tag{8}$$

where ε_n^c and ε_n^h (ε_m^h and ε_m^c) are the initial and final energy eigenvalues along the compression (expansion), respectively; $n(t)$ and $m(t)$ are integers indicating the states occupied by the system at time t. The state $|n(t_0)\rangle$ is independent of the state $|m(\tau_\alpha)\rangle$, because the system that has reached the unique periodic steady state is much closer to thermal equilibrium at the end of the hot or cold isochore. Therefore, the probability density of the stochastic work can be obtained as follows [18]:

$$p(w) = \sum_{n,m} p_n(0) p_m(\tau_c) \delta\{w - w[n(0); m(\tau_c)]\}. \tag{9}$$

This allows us to determine all moments of stochastic work as follows: $\langle w^k \rangle = \int w^k p(w) dw$ ($k = 1, 2, \dots$). Consequently, using Eq. (8), the average work done per cycle $\langle w \rangle$ can be

expressed as follows:

$$\langle w\rangle = \int w p(w) dw = \sum_n \left(\varepsilon_n^h - \varepsilon_n^c\right)[p_n(0) - p_n(\tau_c)]. \quad (10)$$

Hence, the stochastic work fluctuations can be numerically determined according to $\langle \delta w^2\rangle = \langle w^2\rangle - \langle w\rangle^2$. Notably, the average power output and power fluctuations are $P = \langle w\rangle/\tau_{\rm cyc}$ and $\delta P^2 = (\langle w^2\rangle - \langle w\rangle^2)/\tau_{\rm cyc}^2$, respectively.

An adiabatic process can be realized [53] when the energy gaps of the system are changed by the same ratio during an adiabatic driven stroke, without consideration to energy quantization [54]. For simplicity, the ground-state energy was selected as the energy reference point, that is, $\varepsilon_0^h = \varepsilon_0^c = 0$, which implies that $\varepsilon_n^h = \lambda\varepsilon_n^c$. By considering Eqs. (7) and (10), the thermodynamic efficiency of the machine can be obtained as follows:

$$\eta = \frac{\langle w\rangle}{\langle q_h\rangle} = 1 - \frac{1}{\lambda}, \quad (11)$$

where $\lambda > 1$ owing to $\varepsilon_n^h > \varepsilon_n^c$.

To better understand the mechanism of performance enhancement in the finite time of the heat engine, we investigate the influence of the ME on the average power and power fluctuations. As an example, let us consider the Otto cycle based on system $\mathcal{S}_1$ or $\mathcal{S}_2$ by fixing the ratio λ and, thus, the efficiency η. While the energy barriers for system $\mathcal{S}_1$ are $\mathcal{B}_{12} = 1.5$, $\mathcal{B}_{13} = 0.8$, and $\mathcal{B}_{23} = 1.2$, the energy barriers for system $\mathcal{S}_2$ are $\mathcal{B}_{12} = 0.2$, $\mathcal{B}_{13} = 1.7$, and $\mathcal{B}_{23} = 1.9$. These two systems have the same energies, which are $\varepsilon_1^c = 0$, $\varepsilon_2^c = 0.1$, and $\varepsilon_3^c = 0.7$. The energies along the hot stroke are $\varepsilon_n^h = \lambda\varepsilon_n^c$, with $\lambda = 5$. When a value of the inverse temperature β_h^r is set to select the initial probability $\overrightarrow{p}^{\,\rm initial}(0)$ and the initial value of the system's inverse temperature $\beta_A^{\rm initial}(= \lambda\beta_h^r)$ at time $t = 0$, the time durations τ_c and τ_h of the two isochores can be numerically determined by using periodic boundary constraints (the details of the calculation can be found in the Appendix).

Figures 2(a) and 2(b) show the plots of the time durations τ_c and τ_h as a function of the hot bath inverse temperature β_h^r for the heat engines based on systems $\mathcal{S}_1$ and $\mathcal{S}_2$, respectively. Although the time required for cooling a system without ME monotonically increases as the hot bath temperature increases, the system allowing for the ME and initiated at a hot temperature cools down faster than an identical system prepared at a cold temperature when both systems are cooling by the colder bath with inverse temperature β_c^r. The time duration τ_c (τ_h) increases with the inverse temperature β_h^r for the heat engine based on system $\mathcal{S}_1$, owing to the ME (inverse ME) when $\beta_h^r \lessapprox 0.42 (\beta_h^r \lessapprox 0.72)$, as shown in Fig. 2(a). However, when $\beta_h^r > 0.42$ ($\beta_h^r > 0.72$), the ME (inverse ME) vanishes [as shown in Fig. 2(a)]. In this region of large β_h^r values, the time duration τ_c or τ_h decreases as β_h^r increases, as shown in Fig. 2(b), where neither the ME nor the inverse ME is present. As can be seen, the time duration of the cooling stroke (τ_c) is larger than one of the heating branch (τ_h), which coincides with the theoretical prediction [55] of the uphill relaxation to equilibrium being faster. The difference between τ_c and τ_h is observed here to be very large, but not necessarily so in general, as the distance function that determines the relaxation

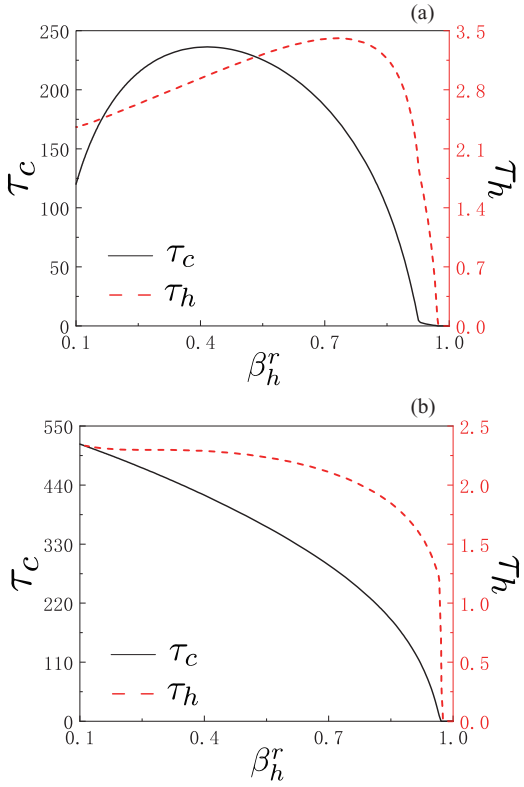

FIG. 2. Time duration spent on two isochores for machines working with systems (a) $\mathcal{S}_1$ and (b) $\mathcal{S}_2$ versus inverse temperature β_h^r. For system $\mathcal{S}_1$, the energy barriers are $\mathcal{B}_{12} = 1.5$, $\mathcal{B}_{13} = 0.8$, and $\mathcal{B}_{23} = 1.2$; for system $\mathcal{S}_2$ the energy barriers are $\mathcal{B}_{12} = 0.2$, $\mathcal{B}_{13} = 1.7$, and $\mathcal{B}_{23} = 1.9$. Systems S_1 and S_2 both have the same energies: $\varepsilon_1^c = 0$, $\varepsilon_2^c = 0.1$, and $\varepsilon_3^c = 0.7$. The energies along the hot stroke are $\varepsilon_n^h = \lambda\varepsilon_n^c$, with $\lambda = 5$. The inverse temperature of the cold thermal bath is $\beta_c^r = 5$.

time sensitively depends on the system parameters. Suppose there is a system [56] that undergoes a cooling process which is the reverse of a heating process. In Eq. (4), $p_n(0)$ and π_n, which are the respective occupation probabilities at the initial and final states for the heating process, can be set as the final and initial probability functions for the cooling process. Clearly the distance function (4) monotonically increases as the bath's inverse temperature β^r when the values of both $p_n(0)$ and π_n are given, and thus the distance function F is larger in the cooling process where $\beta^r = \beta_c^r$ than in the heating one with $\beta^r = \beta_h^r$. By comparing Figs. 2(a) and 2(b), it can be seen that the cooling time of system $\mathcal{S}_1$ is smaller than that of $\mathcal{S}_2$. However, this is not always the case, because the time for the cooling process depends on the selected system parameters, such as the energies, the energy barriers, and the initial temperature.

On the basis of the above discussion, we can now explore the ME in the work and the power statistics of the thermal machine. The average work and work fluctuations of the machine working system $\mathcal{S}_1$ with ME and system $\mathcal{S}_2$ without the ME for different efficiencies η [Eq. (11)] are shown in Figs. 3(a) and 3(b), respectively. For given β_c^r, the average work and work fluctuations increase as the hot bath inverse temperature β_h^r decreases, regardless of whether ME is present. This can

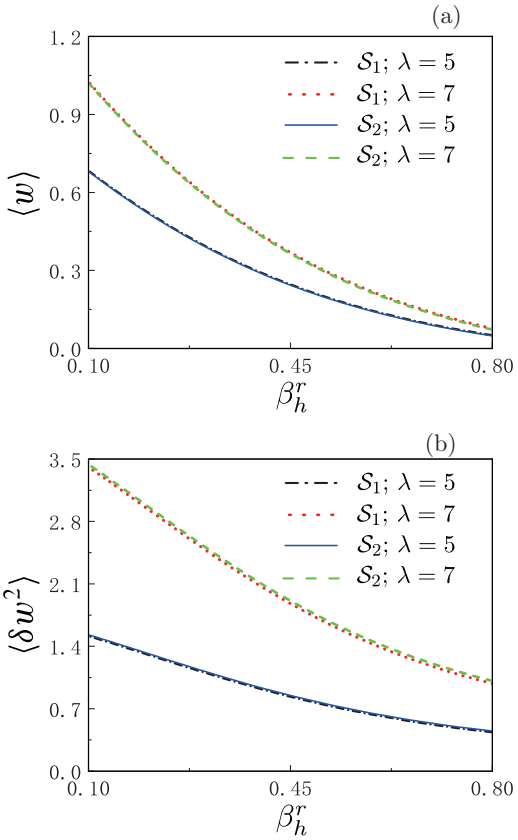

FIG. 3. (a) Average work $\langle w \rangle$ and (b) work fluctuations $\langle \delta w^2 \rangle$ versus inverse temperature β_h^r for $\lambda = 5$ and $\lambda = 7$. The other parameters are the same as those in Fig. 2.

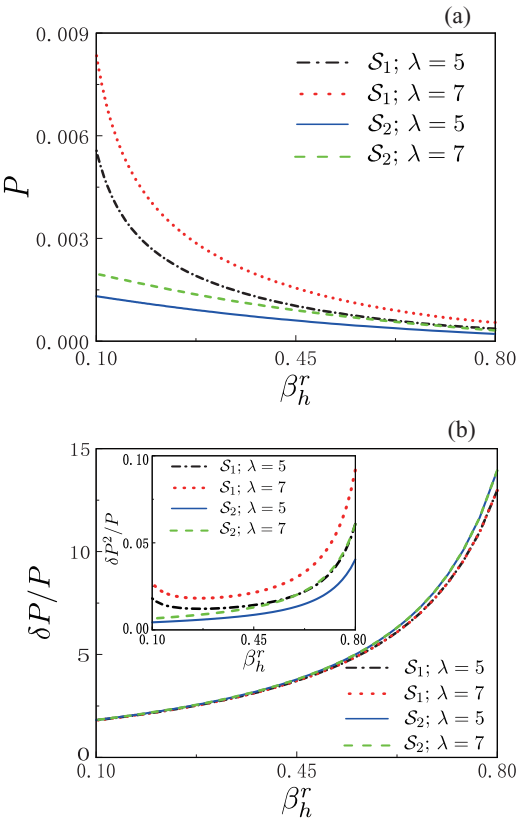

FIG. 4. (a) Average power P and (b) square root of relative power fluctuations $\delta P/P$ versus inverse temperature β_h^r for $\lambda = 5$ and $\lambda = 7$. The inset in panel (b) shows the Fano factor $\delta P^2/P$ as a function of inverse temperature β_h^r. The other parameters are the same as those in Fig. 2.

be understood by the fact that the increase of the difference between the two bath temperatures increases the average work and fluctuations. Notably, when λ is given, the average work produced by the machine with the ME and the machine without the ME collapses into a single line, and a similar behavior holds in the work fluctuations. This follows from the fact that the stochastic work given by Eq. (8) depends on the system energies only, and the effects induced by the energy barriers, which account for the ME in our model, are entered into the work distribution function [Eq. (9)] (if the system reaches the thermal equilibrium, $\vec{p}\,(t \to \infty) = \vec{\pi}$, the effects exerted by the energy barriers disappear).

The comparison of the power output of the engine based on system $\mathcal{S}_1$ to that produced by system $\mathcal{S}_2$ is shown in Fig. 4(a) as a function of the inverse temperature β_h^r. In Fig. 4(a), it can be seen that, as β_h^r decreases, the power output produced by system $\mathcal{S}_1$ exponentially increases in the region ($\beta_h^r \lessapprox 0.42$) where the ME exists [Fig. 2(a)]. The power output produced by system $\mathcal{S}_1$ when $\beta_h^r > 0.42$ or by system $\mathcal{S}_2$ decreases almost linearly as β_h^r increases because the ME is absent in both of these cases. In physical terms, the decrease of the hot bath inverse temperature β_h^r increases the average work $\langle w \rangle$, but a considerable speedup in the cooling process can be generated in the presence of the ME and will thereby exponentially increase the power output P. Hence for the selected parameters of system $\mathcal{S}_1$, the ME may be an important factor for improving the machine performance because the ME can significantly enhance the power output without sacrificing the thermodynamic efficiency.

Finally, the stability of the machine is analyzed by comparing system $\mathcal{S}_1$, where the ME may occur, to system $\mathcal{S}_2$ without the ME. The machine stability can be described by the Fano factor for work $\langle \delta w^2 \rangle / \langle w \rangle$, which is determined by the ratio of work fluctuations $\langle \delta w^2 \rangle$ to the average work $\langle w \rangle$, or the coefficient of variation for work $\langle \delta w \rangle / \langle w \rangle$, which is equal to the square root of the relative power fluctuations, $\delta P/P$. These two are measures for the dispersion of the probability distribution [24] and describe similar physics. Here, we consider the coefficient of variation because it is dimensionless, and we plot this coefficient as a function of the inverse temperature β_h^r in Fig. 4(b). As can be seen, the values of the coefficient $\delta P/P$ for different values of λ collapse to a single form and are thus independent of the efficiency η. In particular, that in the region where the ME occurs under the influence induced by the ME on the coefficient of variation $\delta P/P$ disappears. Although the Fano factor $\delta P^2/P$ is larger in the presence of the ME compared with that without the ME [see inset of Fig. 4(b)], the power fluctuations follow super-Poisson statistics owing to the Fano factor $\delta P^2/P < 1$, which indicates that the engine with ME runs in the stable regime.

Before ending this section, we would like to mention that here we consider only one of the many periodic states that the machine could explore, in which the system is close to thermal

equilibrium at the end of the isochoric process. This leaves a large amount of configurations of the heat engine unexplored and limits the generality of these results.

IV. CONCLUSIONS

This study considered the finite-time performance and the stability of an Otto engine working with two different systems: one system wherein the ME may exist and another system without the ME. Under the condition of the engine having reached the unique, periodic steady state, the time periods (τ_c and τ_h) of the isochoric cooling and heating strokes were numerically determined by assuming the distance function to be much closer to zero. The observation of τ_h being much less than τ_c, regardless of the presence or the absence of the ME, coincides with the theoretical prediction of the asymmetric relaxation. It was discovered that the ME can significantly boost the power output without increasing the relative power fluctuations and sacrificing the machine efficiency. Finally, it was found that the influence induced by the ME on the relative power fluctuations is negligible, and the engine with the ME is stable owing to the very small super-Poisson Fano factor for power.

ACKNOWLEDGMENTS

This work is supported by the National Science Foundation of China (Grants No. 11875034 and No. 11935010) and the Opening Project of Shanghai Key Laboratory of Special Artificial Microstructure Materials and Technology.

APPENDIX: NUMERICAL METHOD FOR DETERMINING THE TIME DURATIONS OF THE TWO ISOCHORIC PROCESSES

Notably, from Eq. (1) in the main text, the probabilities $\overrightarrow{p}(t)$ at any instants during the isochore of the machine under consideration can be determined as follows:

$$\overrightarrow{p}(t) = \exp(\overrightarrow{R}_c t)\overrightarrow{p}(0), \tag{A1}$$

with $0 \leqslant t \leqslant \tau_c$. Here, the transition rate matrix is expressed as

$$\overrightarrow{R}_c = \begin{pmatrix} \bullet & R_{12} & R_{13} \\ R_{21} & \bullet & R_{23} \\ R_{31} & R_{32} & \bullet \end{pmatrix},$$

where the off-diagonal elements $(R_{nm})_{n\neq m}$ and the diagonal elements R_{nn} are determined by Eq. (2) with γ replaced by γ_c and β^r replaced by β_c^r. Because the occupation probability $\overrightarrow{p}$ is kept constant along the isentropic, adiabatic process, the evolution of the probabilities $\overrightarrow{p}(t)$ along the hot isochore with $\tau_c \leqslant t \leqslant \tau_c + \tau_h$ is given by the following equation:

$$\overrightarrow{p}(t) = \exp(\overrightarrow{R}_h t)\overrightarrow{p}(\tau_c), \tag{A2}$$

where the elements R_{nm} are determined according to Eq. (2) by replacing γ and β^r with γ_h and β_h^r, respectively. A single cycle is performed, according to the state evolution along the two isochoric strokes described by Eqs. (A1) and (A2); that is, the evolution of the system for one cycle is given by the following equation:

$$\overrightarrow{p}(\tau_h + \tau_c) = \overrightarrow{M}\overrightarrow{p}(0), \tag{A3}$$

where $\overrightarrow{M} = \exp(\overrightarrow{R}_c \tau_c)\exp(\overrightarrow{R}_h \tau_h)$ is used.

The system evolution over many cycles is determined by the repeated application of the positive transition matrix $\overrightarrow{M}$, which indicates that the system evolves to a periodic steady state after infinite cycles [51],

$$\overrightarrow{p}^{\,\mathrm{ps}}(0) = \lim_{i\to\infty} \overrightarrow{M}^i \overrightarrow{p}(0). \tag{A4}$$

This implies that the following equation holds:

$$\overrightarrow{p}^{\,\mathrm{ps}}(0) = \overrightarrow{M}\overrightarrow{p}^{\,\mathrm{ps}}(0). \tag{A5}$$

For a machine where the inverse temperatures of two baths (β_c^r and β_h^r) are given, our numerical approach for determining the times τ_c and τ_h is as follows. First, we choose the initial value of the probability at the beginning of the cold isochoric stroke by setting $\overrightarrow{p}^{\,\mathrm{initial}}(0) = \overrightarrow{\pi}(\beta_h^r)$ due to constant entropy, such that we can solve $F[\overrightarrow{p}(\tau_c); \beta_c^r] \approx 0$ with the precision up to 10^{-4} [see time-dependent distance function F in Figs. 1(c) and 1(d)] with this accuracy indicating that the system is much closer to thermal equilibrium. The initial value of the effective temperature of the system at the

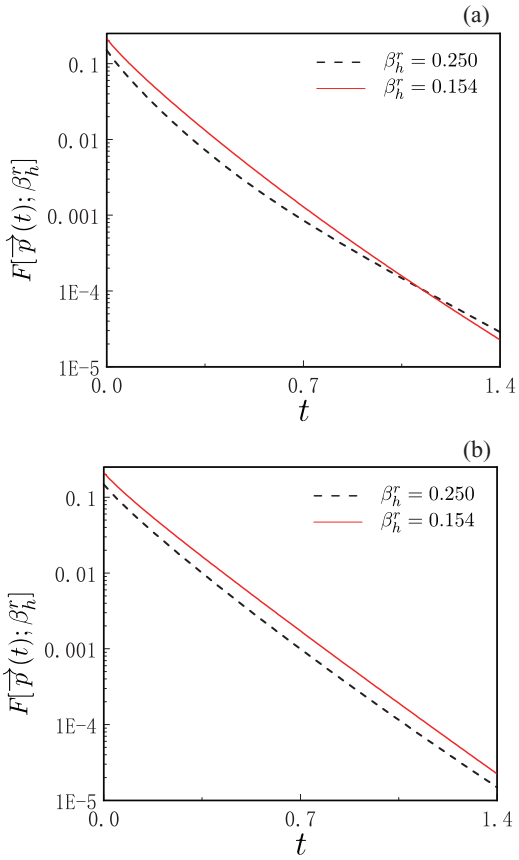

FIG. 5. Distance-from-equilibrium function in heating stroke for machines with systems (a) $\mathcal{S}_1$ and (b) $\mathcal{S}_2$ versus time duration of the system-bath interaction interval. A logarithmic scale is used in the distance function (ordinate axis). The parameters are the same as those in Fig. 2.

beginning of cold isochore [in Fig. 1(e)] is given by $\beta_A^{\text{initial}} = \lambda\beta_h^r$. Moreover, by using Eq. (A1), we can determine $\overrightarrow{p}(\tau_c)$, which is equal to the probability of the system at the initial state of the hot isochore. The next step is to numerically obtain τ_h by determining the root of the equation $F[\overrightarrow{p}(\tau_h); \beta_h^r] \approx 0$ with precision limit 10^{-7} [57] ($F[\overrightarrow{p}(\tau_h), \beta_h^r]$ is plotted in Fig. 5). In the same manner as in the cold isochore, the system is close to the thermal equilibrium at the end of the isochore. Third, the two abovementioned steps are repeated until $\overrightarrow{p}(0)$ approaches its asymptotic value, which indicates that the system reaches the periodic steady state, yielding the value of $\overrightarrow{p}^{\text{ps}}(0)$ in Eq. (A4) and the value of $\overrightarrow{p}^{\text{ps}}(\tau_c)$ in Eq. (A1). Finally, τ_c and τ_h are calculated based on Eq. (A5) using the same approach as in steps one and two. To keep the notation simple, we use $\overrightarrow{p}(t)$ instead of $\overrightarrow{p}^{\text{ps}}(t)$ to describe the periodic steady state in the main text. As emphasized, there are many other periodic steady states that the machine could operate in finite time, in these states the times $\tau_{c,h}$ are determined by setting the distance function F to be finite values (much larger than the precision used here). Since the machine under consideration is set to wait quite long time durations τ_h and τ_c until the distance function is much closer to zero, only one of many periodic states that the machine could explore is considered here.

[1] F. L. Curzon and B. Ahlborn, Efficiency of a Carnot engine at maximum power output, Am. J. Phys. **43**, 22 (1975).

[2] C. Van den Broeck, Thermodynamic Efficiency at Maximum Power, Phys. Rev. Lett. **95**, 190602 (2005).

[3] M. Esposito, R. Kawai, K. Lindenberg, and C. Van den Broeck, Efficiency at Maximum Power of Low-Dissipation Carnot Engines, Phys. Rev. Lett. **105**, 150603 (2010).

[4] A. Ryabov and V. Holubec, Maximum efficiency of steady-state heat engines at arbitrary power, Phys. Rev. E **93**, 050101(R) (2016).

[5] R. Kosloff, Quantum thermodynamics: A dynamical viewpoint, Entropy **15**, 2100 (2013).

[6] R. Kosloff and A. Levy, Quantum heat engines and refrigerators: Continuous devices, Annu. Rev. Phys. Chem. **65**, 365 (2014).

[7] R. S. Whitney, Most Efficient Quantum Thermoelectric at Finite Power Output, Phys. Rev. Lett. **112**, 130601 (2014).

[8] Q. Wang, Performance of quantum heat engines under the influence of long-range interactions, Phys. Rev. E **102**, 012138 (2020).

[9] Z. C. Tu, Efficiency at maximum power of Feynman's ratchet as a heat engine, J. Phys. A **41**, 312003 (2008).

[10] Y. Y. Hong, Y. L. Xiao, J. Z. He, and J. H. Wang, Quantum Otto engine working with interacting spin systems: Finite power performance in stochastic thermodynamics, Phys. Rev. E **102**, 022143 (2020).

[11] Q. Liu, J. Z. He, Y. L. Ma, and J. H. Wang, Finite-power performance of quantum heat engines in linear response, Phys. Rev. E **100**, 012105 (2019).

[12] T. Denzler and E. Lutz, Efficiency fluctuations of a quantum heat engine, Phys. Rev. Res. **2**, 032062(R) (2020).

[13] U. Seifert, Stochastic thermodynamics, fluctuation theorems and molecular machines, Rep. Prog. Phys. **75**, 126001 (2012).

[14] K. Sekimoto, *Stochastic Energetics* (Springer, Berlin, 2010).

[15] M. Esposito, U. Harbola, and S. Mukamel, Nonequilibrium fluctuations, fluctuation theorems, and counting statistics in quantum systems, Rev. Mod. Phys. **81**, 1665 (2009).

[16] M. Campisi, P. Hänggi, and P. Talkner, Colloquium. Quantum fluctuation relations: Foundations and applications, Rev. Mod. Phys. **83**, 771 (2011).

[17] S. Kheradsoud, N. Dashti, M. Misiorny, P. P. Potts, J. Splettstoesser, and P. Samuelsson, Power, efficiency and fluctuations in a quantum point contact as steady-state thermoelectric heat engine, Entropy **21**, 777 (2019).

[18] G. Jiao, S. Zhu, J. He, Y. Ma, and J. Wang, Fluctuations in irreversible quantum Otto engines, Phys. Rev. E **103**, 032130 (2021).

[19] F. Liu and S. H. Su, Stochastic floquet quantum heat engines and stochastic efficiencies, Phys. Rev. E **101**, 062144 (2020).

[20] J. Ren, P. Hänggi, and B. W. Li, Berry-Phase-Induced Heat Pumping and Its Impact on the Fluctuation Theorem, Phys. Rev. Lett. **104**, 170601 (2010).

[21] Z. Wang, L. Q. Wang, J. Z. Chen, C. Wang, and J. Ren, Geometric heat pump: Controlling thermal transport with time-dependent modulations, Front. Phys. **17**, 13201 (2022).

[22] J. Goold, U. Poschinger, and K. Modi, Measuring the heat exchange of a quantum process, Phys. Rev. E **90**, 020101(R) (2014).

[23] S. Pal, S. T. Mahesh, and K. B. Agarwalla, Experimental demonstration of the validity of quantum heat exchange fluctuation relation in NMR setup, Phys. Rev. A **100**, 042119 (2019).

[24] Q. Bouton, J. Nettersheim, S. Burgardt, D. Adam, E. Lutz, and A. Widera, A quantum heat engine driven by atomic collisions, Nat. Commun. **12**, 2063 (2021).

[25] P. Pietzonka and U. Seifert, Universal Trade-Off Between Power, Efficiency, and Constancy in Steady-State Heat Engines, Phys. Rev. Lett. **120**, 190602 (2018).

[26] N. Shiraishi, K. Saito, and H. Tasaki, Universal Trade-Off Relation Between Power and Efficiency for Heat Engines, Phys. Rev. Lett. **117**, 190601 (2016).

[27] Aristotle, *Meteorologica*, translated by H. D. P. Lee (Harvard University, Cambridge, MA, 1962), Book I, Chap. XII, pp. 85–87.

[28] E. B. Mpemba and D. G. Osborne, Cool? Phys. Educ. **4**, 172 (1969).

[29] M. Jeng, The Mpemba effect: When can hot water freeze faster than cold? Am. J. Phys. **74**, 514 (2006).

[30] Z. Lu and O. Raz, Nonequilibrium thermodynamics of the Markovian Mpemba effect and its inverse, Proc. Natl. Acad. Sci. USA **114**, 5083 (2017).

[31] I. Klich, O. Raz, O. Hirschberg, and M. Vucelja, Mpemba Index and Anomalous Relaxation, Phys. Rev. X **9**, 021060 (2019).

[32] A. Kumar and J. Bechhoefer, Exponentially faster cooling in a colloidal system, Nature (London) **584**, 64 (2020).

[33] P. A. Greaney, G. Lani, G. Cicero, and J. C. Grossman, Mpemba-like behavior in carbon nanotube resonators, Metall. Mater. Trans. A **42**, 3907 (2011).

[34] A. Lasanta, F. Vega Reyes, A. Prados, and A. Santos, When the Hotter Cools More Quickly: Mpemba Effect in Granular Fluids, Phys. Rev. Lett. **119**, 148001 (2017).

[35] Y.-H. Ahn, H. Kang, D.-Y. Koh, and H. Lee, Experimental verifications of Mpemba-like behaviors of clathrate hydrates, Korean J. Chem. Eng. **33**, 1903 (2016).

[36] C. Hu, J. Li, S. Huang, H. Li, C. Luo, J. Chen, S. Jiang, and L. An, Conformation directed Mpemba effect on polylactide crystallization, Cryst. Growth Des. **18**, 5757 (2018).

[37] T. Keller, V. Torggler, S. B. Jäger, S. Schütz, H. Ritsch, and G. Morigi, Quenches across the self-organization transition in multimode cavities, New J. Phys. **20**, 025004 (2018).

[38] M. Baity-Jesi *et al.* The Mpemba effect in spin glasses is a persistent memory effect, Proc. Natl. Acad. Sci. USA **116**, 15350 (2019).

[39] F. Vega Reyes, A. Santos, and G. M. Kremer, Role of roughness on the hydrodynamic homogeneous base state of inelastic spheres, Phys. Rev. E **89**, 020202(R) (2014).

[40] A. Torrente, M. A. López-Castaño, A. Lasanta, F. V. Reyes, A. Prados, and A. Santos, Large Mpemba-like effect in a gas of inelastic rough hard spheres, Phys. Rev. E **99**, 060901(R) (2019).

[41] A. Biswas, V. V. Prasad, O. Raz, and R. Rajesh, Mpemba effect in driven granular Maxwell gases, Phys. Rev. E **102**, 012906 (2020).

[42] Z. Y. Yang and J. X. Hou, Non-Markovian Mpemba effect in mean-field systems, Phys. Rev. E **101**, 052106 (2020).

[43] J. P. S. Paterson, T. B. Batalhão, M. Herrera, A. M. Souza, R. S. Sarthour, I. S. Oliveira, and R. M. Serra, Experimental Characterization of a Spin Quantum Heat Engine, Phys. Rev. Lett. **123**, 240601 (2019).

[44] R. Kosloff and Y. Rezek, The quantum harmonic Otto cycle, Entropy **19**, 136 (2017).

[45] M. Campisi, J. Pekola, and R. Fazio, Nonequilibrium fluctuations in quantum heat engines: Theory, example, and possible solid state experiments, New J. Phys. **17**, 035012 (2015).

[46] V. Singh and Ö. E. Müstecaplıoğlu, Performance bounds of nonadiabatic quantum harmonic Otto engine and refrigerator under a squeezed thermal reservoir, Phys. Rev. E **102**, 062123 (2020).

[47] Y. C. Zhang, J. C. Guo, and J. C. Chen, Unified trade-off optimization of quantum Otto heat engines with squeezed thermal reservoirs, Quantum Inf. Process. **19**, 268 (2020).

[48] M. Esposito and C. Van den Broeck, Three faces of the second law. I. Master equation formulation, Phys. Rev. E **82**, 011143 (2010).

[49] S. Kullback and R. A. Leibler, On information and sufficiency, Ann. Math. Stat. **22**, 79 (1951).

[50] T. Schmiedl and U. Seifert, Efficiency at maximum power: An analytically solvable model for stochastic heat engines, Europhys. Lett. **81**, 20003 (2008).

[51] D. Mandal, H. T. Quan, and C. Jarzynski, Maxwell's Refrigerator: An Exactly Solvable Model, Phys. Rev. Lett. **111**, 030602 (2013).

[52] O. Raz, Y. Subaşı, and C. Jarzynski, Mimicking Nonequilibrium Steady States with Time-Periodic Driving, Phys. Rev. X **6**, 021022 (2016).

[53] H. T. Quan, Y. X. Liu, C. P. Sun, and F. Nori, Quantum thermodynamic cycles and quantum heat engines, Phys. Rev. E **76**, 031105 (2007).

[54] D. Gelbwaser-Klimovsky, A. Bylinskii, D. Gangloff, R. Islam, A. Aspuru-Guzik, and V. Vuletic, Single-Atom Heat Machines Enabled by Energy Quantization, Phys. Rev. Lett. **120**, 170601 (2018).

[55] A. Lapolla and A. Godec, Faster Uphill Relaxation in Thermodynamically Equidistant Temperature Quenches, Phys. Rev. Lett. **125**, 110602 (2020).

[56] To further confirm that the asymmetric relaxation to equilibrium holds in the system under consideration, we consider a refrigerator which performs the Otto cycle in a direction opposite to that of the present heat engine. That is, the refrigerator is the reverse of the heat engine under consideration, with the same chosen system parameters. Our additional calculations for determining the total cycle period of the refrigerator show that heating a system is also faster than cooling an identical system. As an example, for $\beta_h^r = 0.2$ (i.e., $\beta_A^{\text{initial}} = \lambda\beta_h^r$ with $\lambda = 5$) and $\beta_c^r = 5$, when $\tau_c = 195.753$ and $\tau_h = 2.532$, τ_c^{re} and τ_h^{re} are calcuated as $\tau_c^{\text{re}} = 2.876$ and $\tau_h^{\text{re}} = 5.563$, where τ_c^{re} (τ_h^{re}) is the time duration of isochoric heating (cooling) in the refrigeration cycle, showing that $\tau_c^{\text{re}} < \tau_c$ and $\tau_h < \tau_h^{\text{re}}$. Here we show that the relaxation time for a given system is larger in a cooling process than in its reverse, but the difference between them does not exist on such a large scale as shown in Fig. 2.

[57] Here we solve $F \approx 0$ by using precision in the heating stroke much higher than that in the cooling process to observe the possible inverse Mpemba effect in the heating process. Even in this case, we find that the time cycle period τ_{cyc} is dominated by τ_c due to the fact that $\tau_c \gg \tau_h$. What would happen if we used the same precision to solve $F \approx 0$?First, when solving $F \approx 0$ with the precision limit 10^{-4}, the values of time τ_h would be smaller than the corresponding values obtained here, and the possible inverse Mpemba effect may not be observed. Second, if we use the precision of 10^{-7} to solve $F \approx 0$ for the cooling process, the values of time τ_c must be larger than the corresponding values in the main text. That is, if we use the same precision to determine the relaxation times τ_c and τ_h, the timescale difference must become larger, and the results obtained here would change quantitatively but not qualitatively.